



## Synthesis of Polyhedral Magnetite Particles by Hydrothermal Process under High Pressure Condition

Siti Machmudah<sup>1,\*</sup>, Wahyudiono<sup>2</sup>, Hideki Kanda<sup>2</sup> & Motonobu Goto<sup>2</sup>

<sup>1</sup>Department of Chemical Engineering, Sepuluh Nopember Institute of Technology, Kampus ITS Sukolilo, Surabaya 60111, Indonesia

<sup>2</sup>Department of Chemical Engineering, Nagoya University, Furo-cho, Chikusa-ku, Nagoya 464-8603, Japan

\*E-mail: machmudah@chem-eng.its.ac.id

**Abstract.** Magnetite particles were successfully generated by hydrothermal synthesis using water at subcritical conditions. By changing the temperature and pressure at subcritical water conditions, the thermodynamics and transport properties of the water can be controlled, thus enabling to manage the way of crystal formation, morphology, and particle size. In this work, the experiments were carried out at temperatures of 250 °C and 290 °C and a pressure of 10 MPa with a reactor made of SUS 316 in a batch system. The synthesized particles were dried in vacuum condition and characterized by SEM and XRD. The XRD patterns showed that magnetite particles were dominantly formed in the particle products with a black color. The results showed that the magnetite particles formed had diameters of around 60 nm in all experiments with irregular polyhedral shaped morphologies.

**Keywords:** magnetite; hydrothermal; subcritical; synthesis; particles.

### 1 Introduction

There are a number oxides from iron that are composed of Fe (iron) together with O (oxygen) and/or OH (hydroxide). Commonly synthesized and versatile iron oxides are magnetite (Fe<sub>3</sub>O<sub>4</sub>), hematite (α-Fe<sub>2</sub>O<sub>3</sub>), maghemite (γ-Fe<sub>2</sub>O<sub>3</sub>), and goethite (α-FeOOH) [1]. Magnetite, one of the common iron oxides, has unique electric and magnetic properties because of the presence of iron cations in two valence states, Fe<sup>2+</sup> and Fe<sup>3+</sup>, in the octahedral sites. This iron oxide has a cubic inverse spinel structure as a common ferrite from iron oxides. Magnetite particles have been widely used in separation processes, heat transfer applications, medical applications, biosensors, dynamic sealing, recovery of metal irons, and so on [2-4]. Due to the wide potential application of magnetite particles, the synthesis of this material has been studied intensively in recent years, which has makes them suitable for diverse applications [5].

Several methods have been reported for the formation of magnetite particles in micro-nano scale, such as thermal decomposition, microemulsion, co-

---

Received February 15<sup>th</sup>, 2016, 1<sup>st</sup> Revision October 11<sup>th</sup>, 2016, 2<sup>nd</sup> Revision December 13<sup>th</sup>, 2016, Accepted for publication December 30<sup>th</sup>, 2016.

Copyright ©2016 Published by ITB Journal Publisher, ISSN: 2337-5779, DOI: 10.5614/j.eng.technol.sci.2016.48.6.8

precipitation, and hydrothermal methods [2,4]. Each method has its advantages and disadvantages, hence it is difficult to choose one as the simplest or the most feasible for use in industrial methods. Co-precipitation is the most conventional and most easy way to produce iron oxides. This method has been shown to be economic and versatile and is being applied in several commercial production plants for the synthesis of magnetite particles. However, controlling the particle size distribution in this method is restricted, because the crystal growth is controlled by kinetic factors. Therefore, a surfactant or stabilizers are needed in the reaction media to generate stabilized nanoparticles [2,4,6]. In thermal decomposition, magnetite particles are synthesized from organometallic compounds in high-boiling organic solvents. This method produces monodispersed particles in nano scale. Nonetheless, the particles formed frequently congregate with a large size distribution. Hence, surfactants are employed to inhibit the growth of the particles and enhance particle stabilization [2,4,7]. Magnetite particles can also be generated by a micro-emulsion consisting of two different immiscible liquids. This method is difficult to control and therefore the particles are produced at a low yield in a relatively wide range of sizes and shapes and require a large amount of solvents. A simple and environmentally friendly method to generate metal oxide particles at micro-nano scale, including iron oxides, is hydrothermal treatment [2,4,8]. The hydrothermal method has advantages such as facility to control particle size and morphology by changing the pressure and temperature of synthesis; applicability to many materials via direct synthesis in the desired crystalline phase at relatively low temperature; and the ability to produce substances in an elemental oxidation state [8].

Although the hydrothermal method has been known as a successful process for the production of crystals of many different materials, a long reaction process is needed when it is conducted at atmospheric pressure [9-11]. Consequently, this method is costly. Fan, *et al.* [9] conducted experiments to produce particles of nanocrystalline magnetite using the hydrothermal method in a simple process at a temperature of 140 °C and atmospheric pressure. They concluded that nanocrystalline magnetite particles were successfully generated from ferrous sulfate, sodium hydroxide and sodium thiosulfate at this condition. However, a long reaction process was required (12 hours). Similar results were obtained in another study on the synthesis of magnetite from ferrous sulfate at a temperature of 180 °C using hydrothermal treatment at atmospheric pressure [11]. The authors state that the morphology of the magnetite particle products was formed in various shapes after 20 hours reaction time. Again, a long reaction time was needed, as can be seen in Table 1. In order to overcome this disadvantage, in the present study, the formation of magnetite particles was conducted using the hydrothermal method at temperatures of 250 °C and 290 °C and a pressure of 10 MPa. This method utilizes the solubility of inorganic substances in water at

subcritical conditions. Due to the change structure of water under elevated temperatures and pressures, it is able to play an important role in the transformation of precursor material and subsequent precipitation of the material dissolved in the fluid [12-14]. The particle products were characterized by SEM and XRD after drying.

**Table 1** Magnetite Synthesis by hydrothermal technique with respect to product morphology.

Operating conditions		Magnetic Source	Products		Reaction time [h]	Reference
T	P		Morphology	Size		
140°C	Ambient	FeSO <sub>4</sub>	quasi-sphere polyhedron	50 nm	12	Fan, <i>et al.</i> [9]
140°C	Ambient	FeCl <sub>2</sub>	quadrangle and hexagon	40 nm	6	Wang, <i>et al.</i> [11]
180°C	Ambient	Fe <sub>3</sub> O(OCOCH <sub>3</sub> ) <sub>6</sub> NO <sub>3</sub> , FeCl <sub>2</sub> ·4H <sub>2</sub> O, FeSO <sub>4</sub> ·7H <sub>2</sub> O	diamond-like, prism-shuttle-like, rod-like and spherical shapes	0.01-12 nm	20	Dong, <i>et al.</i> [10]

## 2 Experimental Section

### 2.1 Materials

The starting material was commercial ferrous sulfate hydrate (FeSO<sub>4</sub>·7H<sub>2</sub>O, Wako Pure Chemical Industries Ltd., Osaka, Japan). Ammonia solution (NH<sub>3</sub>, 28%), hydrogen peroxide (H<sub>2</sub>O<sub>2</sub>, JIS standard), and ethanol (C<sub>2</sub>H<sub>6</sub>O, 99.5%) were purchased from Wako Pure Chemical Industries Ltd. (Osaka, Japan). Distilled-deionized water was produced by a water distillation and water purification apparatus (Shibata Co. model PW-16, Japan. Simplicity UV, Millipore Corp., USA) was used as a solvent throughout the experiments.

### 2.2 Experimental Setup and Procedure

The typical experimental procedure was as follows: 1.5 g ferrous sulfate hydrate was dissolved in 12 ml of distilled-deionized water. After that, 2 ml diluted ammonia (2.5%) was mixed with the solution and stirred around 5 min. Then 0.054 ml hydrogen peroxide was added into the solution slowly while stirring. This solution was stirred for 5 min to obtain a homogeneous condition. Figure 1 shows the general work of magnetite particle synthesis by hydrothermal process. Next, the solution was transferred into a reactor (8.8 ml of volume, SUS 316, AKICO, Japan), sealed and heated at 250 °C and 290 °C [15-17]. The reactor was allowed to work at a temperature of 300 °C and a pressure of 30 MPa. The experiments were conducted at a controlled temperature in batch

reactors. Argon gas was employed to remove air from the reactor prior to sealing it. An electric furnace (ISUZU Co. Ltd., model NMF-13AD, see Figure 2) with temperature controller was used to heat the reactor to the desired temperature.

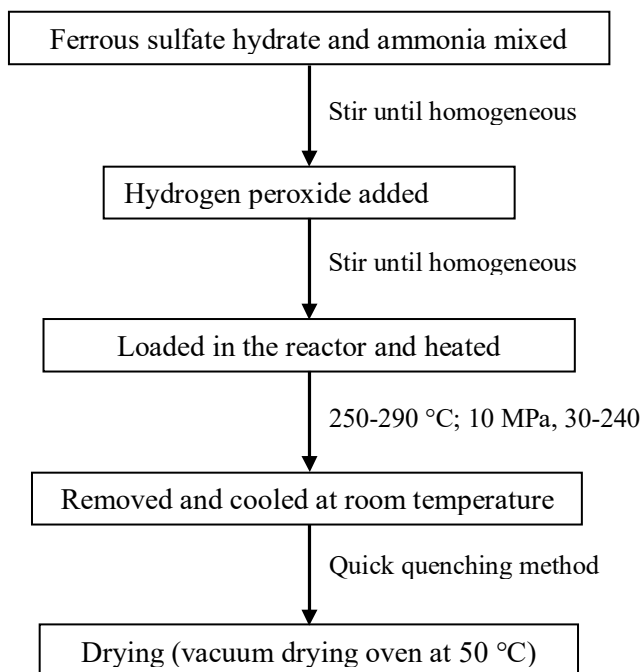


**Figure 1** Flowchart summary of magnetite particle synthesis by hydrothermal process.

In preliminary experiments, the inside temperature of the reactor was determined by a thermocouple (K-type) placed in the reactor. The time needed was 10 min to increase the reactor temperature from ambient to the desired condition so the reactor temperature was similar to the temperature of the furnace. The temperature profile is plotted in Figure 3. In further experiments, the thermocouple was not employed in order to obtain an accurate analysis and complete recovery of the synthesized particle products and to accurately determine the volume of the reactor. The water densities and steam table data were used to estimate the reactor pressures. A mechanical device was applied to shake the reactor during the experiments. The experiments were carried out for 30-240 min (inclusive 10 min of heating time); next, the reactor was removed from the furnace and immediately cooled in a water bath at room temperature. After quenching, the liquid and solid fractions were unloaded from the reactor

and collected by cleaning the inside of the reactor with ethanol. Each experiment was performed in duplicate or triplicate.

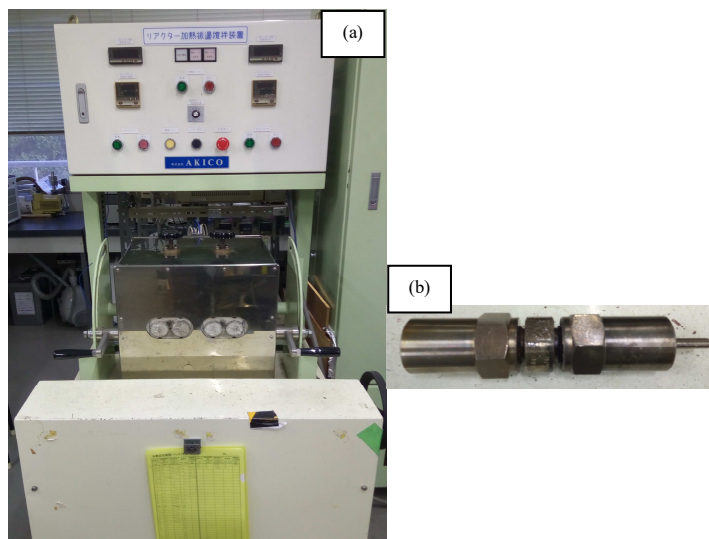


**Figure 2** Electric furnace (a) and SUS reactor (b) used in the experiment.

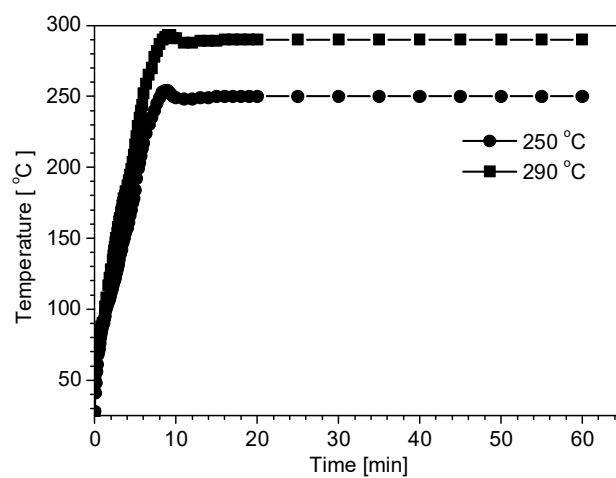


**Figure 3** Typical temperature profile for hydrothermal synthesis at a pressure of 10 MPa.

The surface morphologies of the magnetite particles were characterized with a scanning electron microscope (SEM; JEOL JSM-6390LV). The magnetite particle size was determined from the SEM images by image analyzer software

(Image J 1.42). X-ray diffraction (XRD) patterns were observed to detect that magnetite particles were generated through the hydrothermal synthesis method. A Rigaku RINT 2100/PC XRD machine (40 kV and 200 mA) installed with a  $\theta$ - $\theta$  wide-angle goniometer and scintillation detector was employed for all XRD observations, with Cu K $\alpha$  radiation ( $\lambda = 1.5406 \text{ \AA}$ ).

### 3 Results and Discussion

Figure 4 shows the typical SEM images of the iron oxide particles synthesized under hydrothermal conditions at 250 °C and 290 °C for 60 min synthesis time. These figures show that the hydrothermal process in which the chemical reactions can take place in aqueous media under high temperature and pressure allows to generate iron oxide particles due to the change in dielectric constant. Hayashi and Hakuta [16] explain that synthesis by hydrothermal method respects the heterogeneous particle synthesis or particle growth in the presence of solvent liquids or mineralizers under high temperature and high pressure from materials that are insoluble at temperatures and pressures lower than 100 °C and 1 atm, respectively. At these conditions, the water acts as a reactant for inorganic nanoparticle synthesis. The water molecules dissociate into H<sup>+</sup> and OH<sup>-</sup>, as illustrated by the ionic product ( $K_w$ ) increase as the temperature increases and reaches its highest value at around 300 °C. When the temperature and pressure increase, the density and dielectric constant of the water also shift. The dielectric constant of water is about 78 at ambient temperature. At this condition, the polar point of inorganic salts exhibits solubility. When the water temperature is raised to 200 °C and 300 °C, the dielectric constants are around 35 and 21, respectively. According to electrostatic theory, the dielectric constant has a notable influence on the synthesis reaction rate. At these conditions, a high water density may also significantly promote the transformation due to the hydration effect of the chemical reaction. Consequently, subcritical water may be used as a suitable reaction medium for particle generation due to the increased reaction rate and, according to nucleation theory, the reduced solubility will result in a high degree of supersaturation.

As shown in Figure 4, most of the particles formed seemed to have irregular polyhedral shaped morphologies; their morphologies can even be said to be nearly spherical in shape [18]. At least 500 different particles were randomly selected and used to estimate the size distribution of the generated particles, as shown in Figure 5.

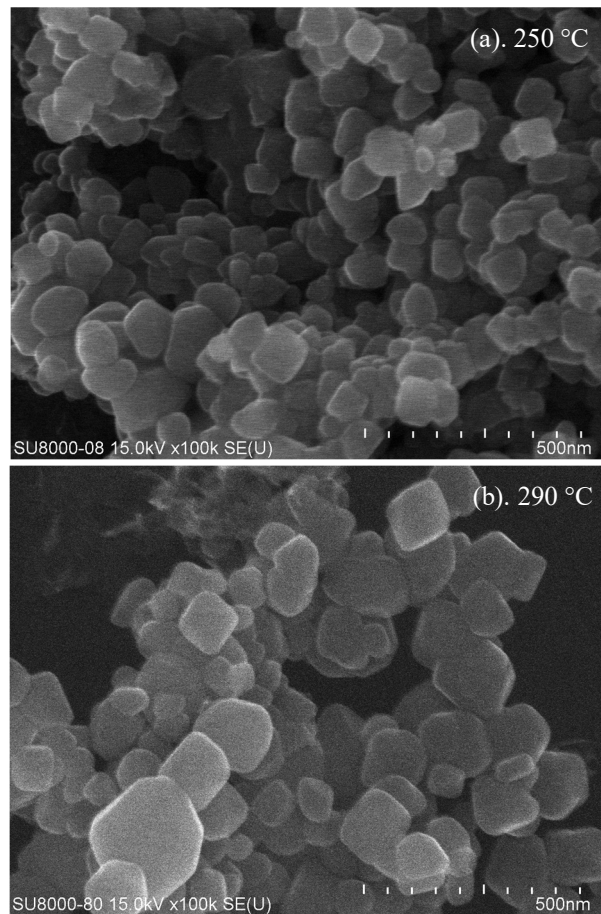


**Figure 4** SEM images of iron oxide particle products at (a) 250 °C and (b) 290 °C, respectively.

Observation showed that the iron oxide particles formed had diameters ranging from 25 to 125 nm. More particularly, most particles generated had 55 nm diameter sizes and fewer particles were found at larger particle sizes (> 100 nm). In this work, the wide range of iron oxide particle diameters indicate that the iron oxide particles were generated via a dissolution and recrystallization process [19]. The big iron oxide particles grow even bigger at the expense of smaller iron oxides particles. This phenomenon, which proceeds according to the Ostwald ripening process, can be explained by the fact that the smaller iron oxide particles in the solution dissolve and precipitate on larger particles in order to reach a more thermodynamically stable state.

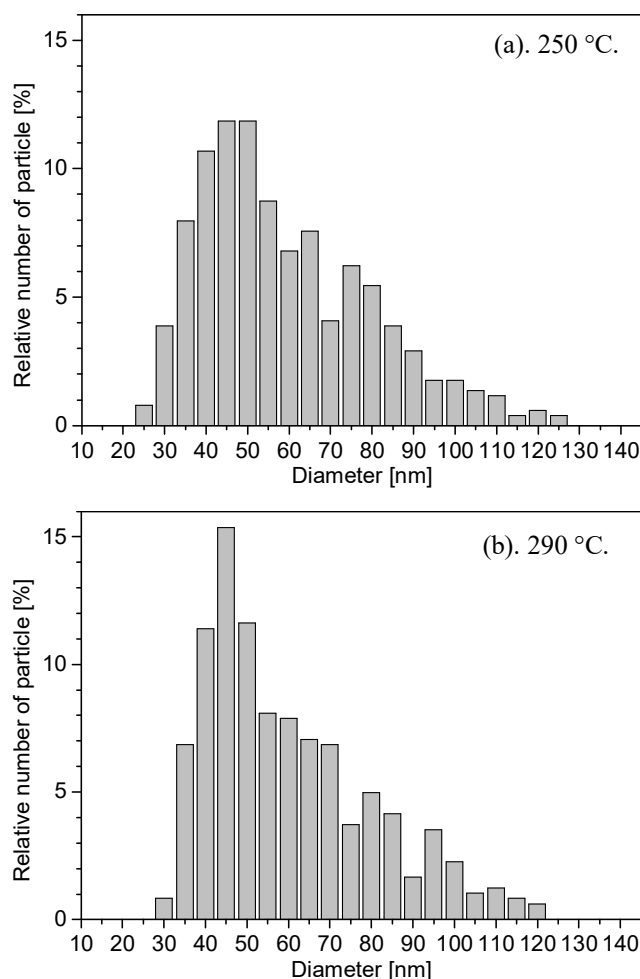


**Figure 5** Particle size distribution of iron oxide particles products at (a) 250 °C and (b) 290 °C, respectively.

In order to know the appearance of the generated particles, the iron oxide particles were observed using XRD [8, 20]. Figures 6(a) and 6(b) illustrate the XRD patterns of the iron oxides particles produced by hydrothermal synthesis at temperatures of 250 °C and 290 °C with 60 minutes synthesis time, respectively. To identify the magnetite formed, the JCPDS system was used. As shown in these figures, the diffraction patterns and relative intensities of all diffraction peaks matched well with those of JCPDS card no. 19-0629 for magnetite [14]. The peak positions and relative intensities of the XRD patterns can be seen at  $2\theta = 30.08^\circ$ ,  $35.42^\circ$ ,  $43.06^\circ$ ,  $56.94^\circ$ ,  $62.52^\circ$  and  $74.96^\circ$ , which are the reflection peaks from the (220), (311), (400), (511), (440) and (533) lattice



planes. These iron oxide particle XRD patterns are in good agreement with the standard magnetite particle XRD patterns [18, 21-25]. At these conditions, the magnetite particles are generated by the following reactions: ferric hydroxide ( $\text{Fe}(\text{OH})_3$ ) is transformed to ferrous hydroxide ( $\text{Fe}(\text{OH})_2$ ) grows on goethite ( $\text{FeOOH}$ ). Then, the complex of ferrous hydroxide-goethite is converted into magnetite [21]. Lian, *et al.* [21] describe in detail that ammonia reacts with water to generate OH radicals at first, which results in a uniform increase of the solution's pH value until the solubility limit. Next, since the solubility product of ferric hydroxide is much lower than that of ferrous hydroxide, with the increase of the pH value, the ferric hydroxide is first precipitated. Then the ferric hydroxide transforms into goethite, which is generally needle-shaped. Due to more hydroxyl ions being generated, the ferrous hydroxide reaches its solubility product. Since there are goethite nucleates, the ferrous hydroxide is allowed to grow on the goethite and finally converted into magnetite. Wei Wu, *et al.* [26] have reported that well-crystallized magnetite grains can also be generated at hydrothermal conditions. In the following process, the crystallized magnetite grains produce increased saturation magnetization in nanosized magnetite.

Sato, *et al.* [25] studied the mechanism of magnetite particle formation using organic compounds to generate magnetite crystals with uncommon facets under hydrothermal conditions. They explain that the magnetite crystal morphology formed by the hydrothermal process of an aqueous solution containing ferrous ions and organic compounds depends on the organic compound used. However, quasi-octahedral magnetite particles can also be produced with water at subcritical conditions and without chemical additives as reaction media. Based on the result, it can be said that the hydrothermal method is a simple and promising route to synthesize magnetite particles. Wei Wu, *et al.* [26] state that the hydrothermal method is prone to generate highly crystalline iron oxides as product results. This method has been applied for single crystal particle growth and nascent generated in hydrothermal synthesis can also have a better crystallinity than those from other methods. Pineiro, *et al.* [27] have reported that the hydrothermal method is an excellent way to generate magnetite particles with high crystallinity. Therefore, the magnetite particles synthesized by this method are very suitable candidates for bioapplications such as targeted drug delivery, magnetic hyperthermia, and MRI contrast agents. It can be said that magnetite particles with high crystallinity possess appropriate performance characteristics for many bioapplications. It should be noted that magnetite is not thermodynamically stable under oxidizing conditions, but nevertheless magnetite will be oxidized to other iron oxides when the environment temperatures are above 400 °C [28].

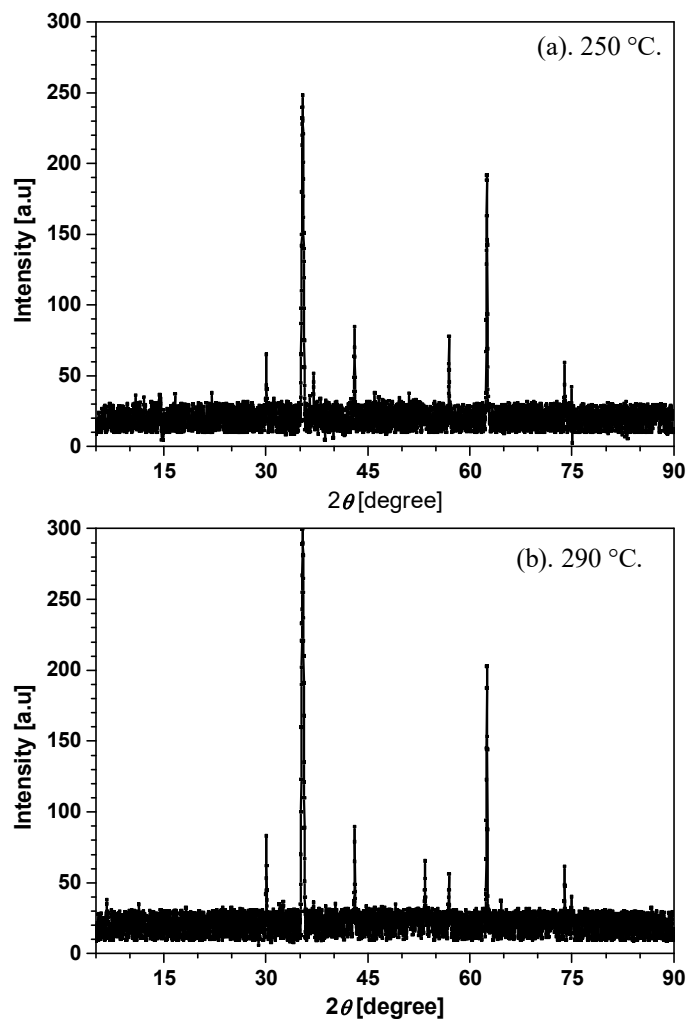


**Figure 6** XRD patterns of iron oxide particles products at (a) 250 °C and (b) 290 °C, respectively.

XRD is the basic technique for characterization of crystal structures and one of the most important non-destructive methods to analyze all types of matter, including fluids, powders, and crystals [14,20]. It can characterize particle products as a whole and provide detailed information from only a few particles. Hosokawa, *et al.* [20] describes the main advantages of using XRD. Firstly, measurements can be conducted in air or atmospheric conditions. Secondly, sample preparation is easier. They also state that the average crystal structures can be evaluated quantitatively. Despite this technique's facility to characterize crystal structures, a broad spectra interpretation and a high noise level in the

spectra baseline may occur (see Figure 6). These phenomena can be found when an XRD with Cu K $\alpha$  radiation is used to characterize material contents with high mass-absorption coefficients, such as iron. A higher and a noisier baseline will be found in the XRD pattern because the sample may emit fluorescent X-rays [29]. As a result, small peaks may be not detected due to the high baseline (background) noise. The average magnetite crystal size can also be determined from the broadening of the XRD line using the Scherrer equation, which shows the corrected width of an XRD line at an angle  $\theta$  as a function of the mean size of the coherently scattering domain perpendicular to the total reflection plane [30]. Due to the relatively high background noise (see Figure 6), both the baseline and the half-width of the XRD peak spectra cannot be determined precisely. This will cause inaccuracy in the determination of the magnetite crystal size. Hence, the magnetite crystal size is not presented in this work.

As mentioned above, the hydrothermal process is simple and can easily produce highly crystalline metal oxides, including magnetite particles, where the size and morphology of the metal oxides particles are prone to be restrained by changing the conditions of synthesis [8,16]. Hayashi and Hakuta [16] explain that the size of metal oxide particles can be controlled by nucleation and grain growth processes during hydrothermal treatment. They state that the temperature and pressure in hydrothermal conditions can be modified in subcritical water to accomplish control of the solvent media during nucleation and crystallization of metal oxide particles. Hence, it can be said that metal oxide particle size is affected by the rate of the hydrolysis reaction and the metal oxide solubility in water media. Machmudah, *et al.* [8] have reported that the diameters of metal oxide particles generated at around 300 °C are clearly larger than the diameters of those generated at 200 °C. Ozel, *et al.* [31] have reported that the diameter of iron oxide nanoparticles increased from  $14.5 \pm 4$  to  $29.9 \pm 9$  nm when the reaction temperature of hydrothermal treatment increased from 100 °C to 180 °C at the same reaction time. Figures 7 and 8 show SEM images of the iron oxide particles generated by hydrothermal treatment at temperatures of 250 °C and 290 °C with various synthesis times. It can be seen in these figures that most of the iron oxide particle products exhibit an irregular polyhedral shaped morphology.

Wang, *et al.* [18] have reported that the solubility and dispersion of substances as starting materials in water at these conditions ( $< 350$  °C) have a large influence on the shape morphology of magnetite formation. If the solubility and dispersion of substances are not properly dissolved and dispersed in the water medium, irregular polyhedral shaped morphologies are generated first. Then they grow into the crystal habit of magnetite according to the Ostwald ripening process. Apparently, their morphology does not change with changing temperature and synthesis time. This is owing to the same growth rate between

the different crystallographic planes of the iron oxide particle products at these temperatures.

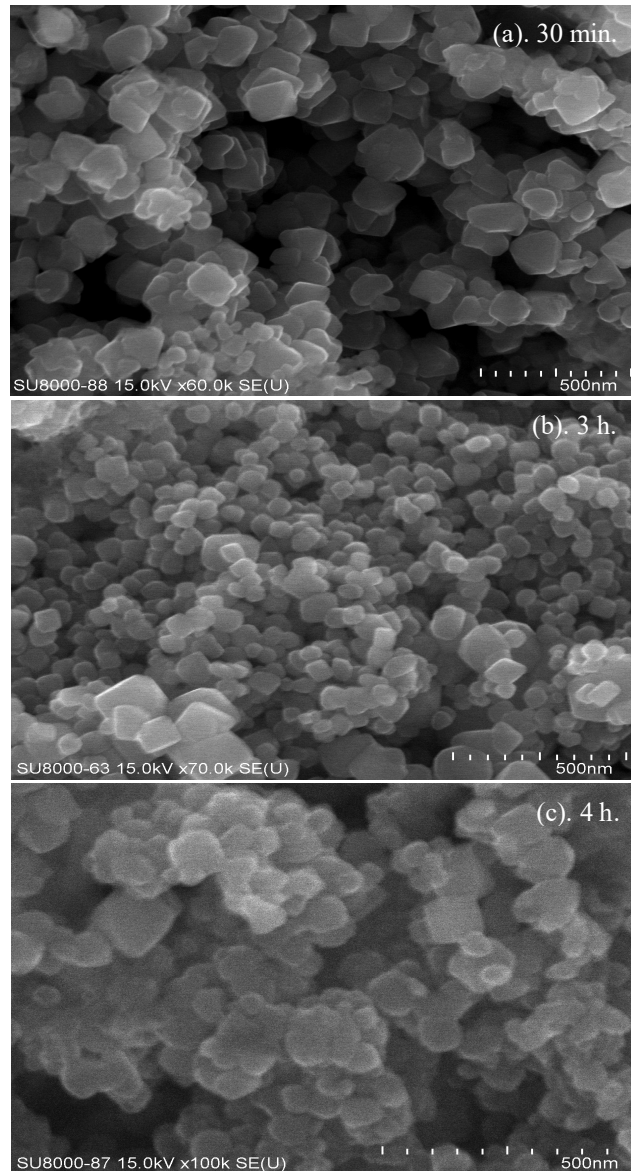


**Figure 7** SEM images of magnetite particle products at 250 °C at various synthesis times.

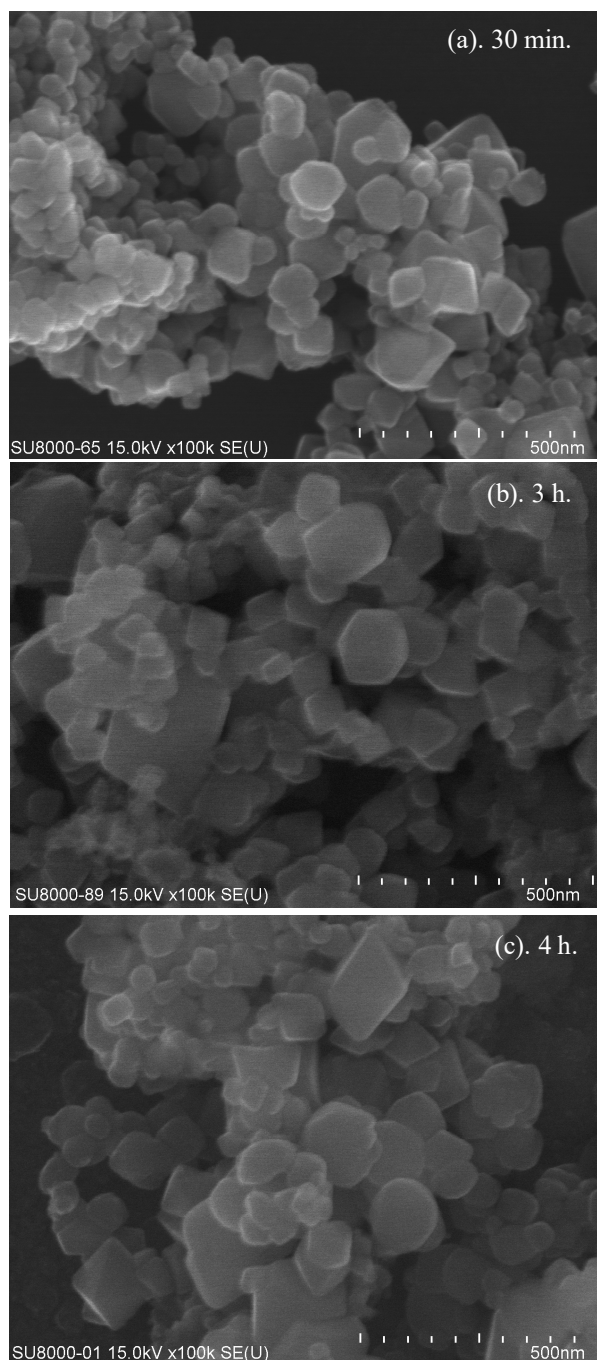


**Figure 8** SEM images of magnetite particles products at 290 °C at various synthesis times.

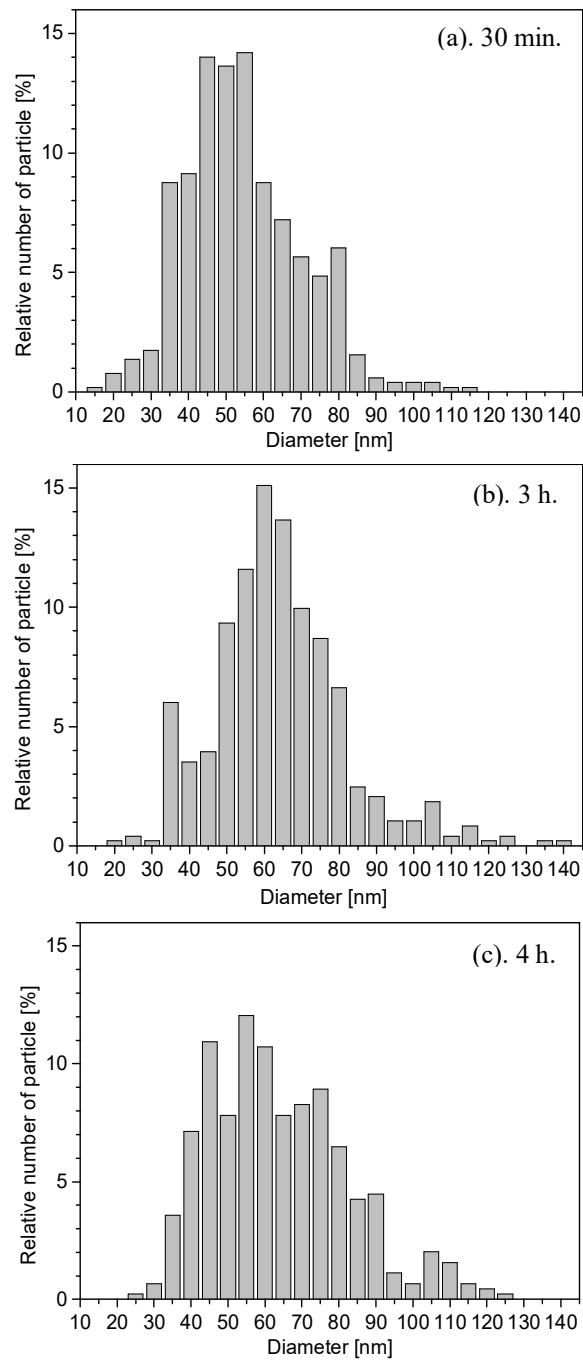


**Figure 9** Particle size distribution of magnetite products at 250 °C at various synthesis times.

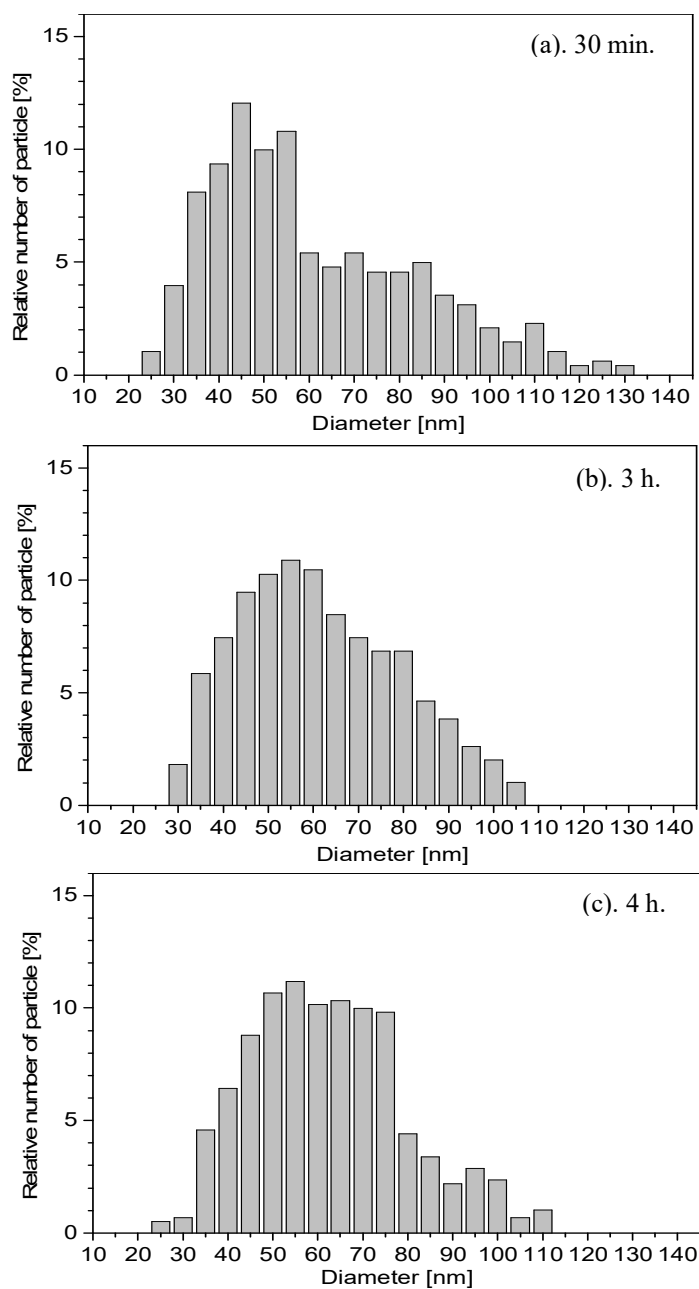


**Figure 10** Particle size distribution of magnetite products at 290 °C at various synthesis times.

In the case of magnetite particle sizes formed, Figures 9 and 10 show the effects of changing temperature and synthesis time on the particle size distribution of the magnetite particles at 250 °C and 290 °C at various synthesis times, respectively. These figures do not show any significant correlation between hydrothermal temperature and synthesis time in the particle size distribution. Nevertheless, it has been known that the hydrothermal reaction in water at subcritical condition has gains for metal oxide compound synthesis due to the increase in reaction rate by several times under conventional hydrothermal conditions (hot water). At this moment, the dielectric constant is low and the metal oxide products have high crystallinity [16]. On average, the magnetite product particle size was 55 nm when the reaction synthesis was carried out at 250 °C with 30 min synthesis time. The average particle size increased to 60 nm when the reaction synthesis was performed at 290 °C with the same synthesis time. This indicates that as the synthesis temperature increases at subcritical water conditions, the solubility of metal oxide, including the iron oxide, is increased until the smaller nano-crystals finally dissolve and re-precipitate the solutes on the bigger nano-crystals [16,18]. Again, this result confirms that the metal oxide particle size depends on the reaction rate and the metal oxide solubility in water at subcritical water conditions. As shown in Figures 9 and 10, the particle size distribution of magnetite products also increased with an increase in synthesis time at the same synthesis temperatures. They increased smoothly with the increase in synthesis time. At these conditions, the nucleation of substances may be quicker than the growth of nascent at elevated temperature and consequently, the particle size decreases. Meanwhile, extending the synthesis time will promote the growth of nascent. As a result, the average magnetite particle product size was around 60 nm at each condition. Therefore, it can be said that the nucleation and crystallization processes of metal particles, which has a large effect on the particle size formed from metal oxide under subcritical water conditions, can be managed by controlling temperature and synthesis time.

#### **4 Conclusions**

Magnetite particles with irregular polyhedral shaped morphologies were synthesized via hydrothermal synthesis. Experiments were conducted in batch process at temperatures of 250 °C and 290 °C and a pressure of 10 MPa. The results did not show any significant correlation between hydrothermal temperature and synthesis time in the particle size distribution of magnetite formed. The particle size of the magnetite formed was 55 nm when the reaction was performed at 250 °C for 30 min and it increased slightly to 60 nm at 290 °C for the same synthesis time. It was found that magnetite products of the same size were obtained when the reaction was conducted at the same reaction temperature with a different synthesis time. Judging by the results, the



hydrothermal synthesis method at subcritical water conditions allows to manage the way of crystal formation, morphology and particle size due to the controllability of the thermodynamics and transport properties via temperature and pressure.

### Acknowledgements

This research was in a collaboration between the Department of Chemical Engineering, Nagoya University, Japan and the Department of Chemical Engineering, Sepuluh Nopember Institute of Technology (ITS), Indonesia.

### References

- [1] Cornell, R.M. & Schwertmann, U., *The Iron Oxides: Structure, Properties, Reactions, Occurrences and Uses*, Wiley-VCH Verlag GmbH & Co. KGaA, Weinheim, Germany, pp. 2-3, 2003.
- [2] Laurent, S., Forge, D., Port, M., Roch, A., Robic, C., Elst, L.V. & Muller, R.N., *Magnetic Iron Oxide Nanoparticles: Synthesis, Stabilization, Vectorization, Physicochemical Characterizations, and Biological Applications*, *Chemical Reviews*, **108**(6), pp. 2064-2110, 2008.
- [3] Mahdavi, M., Ahmad, M.B., Haron, Md.J., Namvar, F., Nadi, B., Rahman, M.Z.Ab. & Amin, J., *Synthesis, Surface Modification and Characterisation of Biocompatible Magnetic Iron Oxide Nanoparticles for Biomedical Applications*, *Molecules*, **18**(7), pp. 7533-7548, 2013.
- [4] Kaur, R., Hasan, A., Iqbal, N., Alam, S., Saini, M. Kr. & Raza, S.K., *Synthesis and Surface Engineering of Magnetic Nanoparticles for Environmental Cleanup and Pesticide Residue Analysis: A Review*, *Journal of Separation Science*, **37**(14), pp. 1805-1825, 2014.
- [5] Wu, W., Wu, Z., Yu, T., Jiang, C. & Kim, W.S., *Recent Progress on Magnetic Iron Oxide Nanoparticles: Synthesis, Surface Functional Strategies and Biomedical Applications*, *Science and Technology of Advanced Materials*, **16**(2), 023501, 2015, doi:10.1088/1468-6996/16/2/023501.
- [6] Durdureanu-Angheluta, A., Pinteala, M. & Simionescu, B.C., *Tailored and Functionalized Magnetite Particles for Biomedical and Industrial Applications in Materials Science and Technology* by Hutagalung, S.D. (Ed.), InTech, Croatia, pp. 150-151, 2012.
- [7] Willard, M.A., Kurihara, L.K., Carpenter, E.E., Calvin, S. & Harris, V.G., *Chemically Prepared Magnetic Nanoparticles*, *International Materials Reviews*, **49**(3-4), pp. 125-170, 2004.
- [8] Machmudah, S., Prastuti, O.P., Widiyastuti, Winardi, S., Wahyudiono, Kanda, H. & Goto. M., *Macroporous Zirconia Particles Prepared by Subcritical Water in Batch and Flow Processes*, *Research on Chemical Intermediates*, **42**(6), pp. 5367-5385, 2016.

- [9] Fan, R., Chen, X.H., Gui, Z., Liu, L. & Chen, Z.Y., *A New Simple Hydrothermal Preparation of Nanocrystalline Magnetite Fe<sub>3</sub>O<sub>4</sub>*, *Materials Research Bulletin*, **36**(3-4), pp. 497-502, 2001.
- [10] Dong, Q., Kumadai, N., Yonesaki, Y., Takei, T. & Kinomura N., *Hydrothermal Synthesis of Fe<sub>3</sub>O<sub>4</sub> Particles with Various Shapes*, *Journal of the Ceramic Society of Japan*, **117**(1368), pp. 881-886, 2009.
- [11] Wang, J., Sun, J., Sun, Q. & Chen, Q., *One-step Hydrothermal Process to Prepare Highly Crystalline Fe<sub>3</sub>O<sub>4</sub> Nanoparticles with Improved Magnetic Properties*, *Materials Research Bulletin*, **38**(7), pp. 1113-1118, 2003.
- [12] Burda, C., Chen, X., Narayanan, R. & El-Sayed, M.A., *Chemistry and Properties of Nanocrystals of Different Shapes*, *Chemical Reviews*, **105**(4), pp. 1025-1102, 2005.
- [13] Wahyudiono, Machmudah, S. & Goto, M., *Utilization of Sub and Supercritical Water Reactions in Resource Recovery of Biomass Wastes*, *Engineering Journal*, **17**(1), pp. 1-9, 2013.
- [14] Machmudah, S., Zuhijah, R., Wahyudiono, Setyawan, H., Kanda, H. & Goto, M., *Magnetite Thin Film on Mild Steel Formed by Hydrothermal Electrolysis for Corrosion Prevention*, *Chemical Engineering Journal*, **268**, pp. 76-85, 2015.
- [15] Rabenau, A., *The Role of Hydrothermal Synthesis in Preparative Chemistry*, *Angewandte Chemie International Edition*, **24**(12), pp. 1026-1040, 1985.
- [16] Hayashi, H. & Hakuta, Y., *Hydrothermal Synthesis of Metal Oxide Nanoparticles in Supercritical Water*, *Materials*, **3**(7), pp. 3794-3817, 2010.
- [17] Bojin, F.M. & Paunescu, V., *Pros and Cons on Magnetic Nanoparticles Use in Biomedicine and Biotechnologies Applications in Nanoparticles' Promises and Risks Characterization, Manipulation, and Potential Hazards to Humanity and the Environment* by Lungu, M., Neculae, A., Bunoiu, M., Biris, C. (Eds.), Springer International, Romania, pp. 103-135, 2015.
- [18] Wang, X., Zhao, Z., Qu, J., Wang, Z. & Qiu, J., *Shape-Control and Characterization of Magnetite Prepared via a One-Step Solvothermal Route*, *Crystal Growth & Design*, **10**(7), pp. 2863-2869, 2010.
- [19] Wang, F. & Wang, X., *Mechanisms in the Solution Growth of Freestanding Two-dimensional Inorganic Nanomaterials*, *Nanoscale*, **6**, pp. 6398-6414, 2014.
- [20] Hosokawa, M., Nogi, K., Naito, M. & Yokoyama, T., *Nanoparticle Technology Handbook*, 1<sup>st</sup> ed., Elsevier, Amsterdam, pp. 270-272, 2007.
- [21] Lian, S., Wang, E., Kang, Z., Bai, Y., Gao, L., Jiang, M., Hu, C. & Xu, L., *Synthesis of Magnetite Nanorods and Porous Hematite Nanorods*, *Solid State Communications*, **129**(8), pp. 485-490, 2004.

- [22] Li, J.H., Hong, R.Y., Li, H.Z., Ding, J., Zheng, Y. & Wei, D.G., *Simple Synthesis and Magnetic Properties of Fe<sub>3</sub>O<sub>4</sub>/BaSO<sub>4</sub> Multi-core/shell Particles*, Materials Chemistry and Physics, **113**(1), pp. 140-144, 2009.
- [23] Cai, W. & Wan, J., *Facile Synthesis of Superparamagnetic Magnetite Nanoparticles in Liquid Polyols*, Journal of Colloid and Interface Science, **305**(2), pp. 366-370, 2007.
- [24] Kokate, M., Garadkar, K. & Gole. A., *One Pot Synthesis of Magnetite-Silica Nanocomposites: Applications as Tags, Entrapment Matrix and in Water Purification*, Journal of Materials Chemistry A, **1**(6), pp. 2022-2029, 2013.
- [25] Sato, J., Kobayashi, M., Kato, H., Miyazaki, T. & Kakihana M., *Hydrothermal Synthesis of Magnetite Particles with Uncommon Crystal Facets*, Journal of Asian Ceramic Societies, **2**(3), pp. 258-262, 2014.
- [26] Wu, W., He, Q. & Jiang, C., *Magnetic Iron Oxide Nanoparticles: Synthesis and Surface Functionalization Strategies*, Nanoscale Research Letters, **3**(11), pp. 397-415, 2008.
- [27] Pineiro, Y., Vargas, Z., Rivas, J. & Lopez-Quintela, M.A., *Iron Oxide Based Nanoparticles for Magnetic Hyperthermia Strategies in Biological Applications*, European Journal of Inorganic Chemistry, **2015** (27), pp. 4495–4509, 2015.
- [28] Colombo, U. Fagherazzi, G., Gazzarrini, F., Lanzavecchia, G. & Sironi, G., *Mechanism of Low Temperature Oxidation of Magnetites*, Nature, **219**, pp. 1036–1037, 1968.
- [29] Namatame, Y., *Making High Speed, High Resolution Measurements using MiniFlex II+D/teX Ultra*, The Rigaku Journal, **27**(1), pp. 6-8, 2011.
- [30] Ingham, B. *X-ray Scattering Characterisation of Nanoparticles*, Crystallography Reviews, **21**(4), pp. 229-303, 2015.
- [31] Ozel, F., Kockar, H. & Karaagac, O., *Growth of Iron Oxide Nanoparticles by Hydrothermal Process: Effect of Reaction Parameters on the Nanoparticle Size*, Journal of Superconductivity and Novel Magnetism, **28**(3), pp. 823-829, 2015.